Continental Shelf Research 156 (2018) 23–32

Contents lists available at ScienceDirect

Continental Shelf Research

journal homepage: www.elsevier.com/locate/csr

On the phase lag of turbulent dissipation in rotating tidal flows

Qianjiang Zhang, Jiaxue Wu*

The Center for Coastal Ocean Science and Technology (CCOST), School of Marine Sciences, Sun Yat-sen University, No. 341 Building, No. 135, Xin Gang Xi Road, Guangzhou 510275, Guangdong, China

ARTICLE INFO

Keywords:
Tidal Ekman bottom boundary layer
Turbulent dissipation
Shear production
Local turbulent kinetic energy balance
Phase lag
Rotating tidal current
Yellow Sea

ABSTRACT

Field observations of rotating tidal flows in a shallow tidally swept sea reveal that a notable phase lag of both shear production and turbulent dissipation increases with height above the seafloor. These vertical delays of turbulent quantities are approximately equivalent in magnitude to that of squared mean shear. The shear production approximately equals turbulent dissipation over the phase-lag column, and thus a main mechanism of phase lag of dissipation is mean shear, rather than vertical diffusion of turbulent kinetic energy. By relating the phase lag of dissipation to that of the mean shear, a simple formulation with constant eddy viscosity is developed to describe the phase lag in rotating tidal flows. An analytical solution indicates that the phase lag increases linearly with height subjected to a combined effect of tidal frequency, Coriolis parameter and eddy viscosity. The vertical diffusion of momentum associated with eddy viscosity produces the phase lag of squared mean shear, and resultant delay of turbulent quantities. Its magnitude is inhibited by Earth's rotation. Furthermore, a theoretical formulation of the phase lag with a parabolic eddy viscosity profile can be constructed. A first-order approximation of this formulation is still a linear function of height, and its magnitude is approximately 0.8 times that with constant viscosity. Finally, the theoretical solutions of phase lag with realistic viscosity can be justified by realistic phase lags of dissipation.

1. Introduction

The bottom boundary layer driven by tidal currents in the coastal/shelf ocean has been long investigated with respect to its turbulence dynamics, because near-bed turbulence is responsible for the vertical transfers of momentum and scalars, erosion and deposition of fine-grained sediments, and associated ecological issues in the coastal/shelf ocean (Grant and Madsen, 1986; Mehta et al., 1989; Yoshikawa et al., 2010). In the tide-dominated estuarine or coastal sea, it has been widely recognized that the time variation of dissipation at a certain height could display a time lag behind that at the seabed (Simpson et al., 1996, 2000; Burgett et al., 2001; Souza et al., 2004). The field observations in the Irish Sea showed that the time lag of dissipation is 1.5 h under the well-mixed conditions from the seabed to the height of 70 m (Simpson et al., 1996). The time lag becomes about 4 h under the stratified conditions from the seabed to the height of 40 m (Simpson et al., 2000). Souza et al. (2004) observed a time lag of about 1 h in shear production at a height of 12 m under the well-mixed conditions in the upper Gulf of California. The phase lag of dissipation affects matter diffusion in the bottom boundary layer (BBL). The field observations in the Western English Channel showed that maximum turbulent dissipation at the base of the thermocline occurred about 5 h after maximum tidal current. This time lag in turbulence mixing aids phytoplankton growth by supplying bottom-layer nutrients into the subsurface chlorophyll maximum (Sharples et al., 2001). The phase lag of suspended sediment concentration has the same magnitude as the phase lag of dissipation (Simpson et al., 2000). The main findings of these studies are that the phase lag of turbulent dissipation is due to that of shear production (Simpson et al., 1996, 2000), and the phase lag of turbulent quantities has a close relationship with the phase lag of squared mean shear (Burgett et al., 2001; Simpson et al., 2000). A one-dimensional (1-d) vertically resolving turbulence closure model, which does not include the vertical diffusion of turbulent kinetic energy (TKE) (i.e. local TKE balance between shear production and dissipation), reproduced the phase lag phenomenon (Simpson et al., 1996). This indicates that the phase delay of dissipation should not be caused by the vertical TKE diffusion.

On the assumption that the phase lag of turbulent dissipation is induced by that of shear production, and the phase lag of two turbulent quantities is caused by the phase lag of squared mean shear, a theoretical formulation for the phase lag of dissipation in the rectilinear tidal current bottom layer has been developed by Simpson et al. (2000) as follows

$$\varphi = \sqrt{\frac{2\omega}{A_z}}z + \frac{\pi}{2}, \tag{1}$$

---

* Corresponding author.
E-mail address: wujiaxue@mail.sysu.edu.cn (J. Wu).

https://doi.org/10.1016/j.csr.2018.02.001
Received 25 April 2017; Received in revised form 20 December 2017; Accepted 4 February 2018

where φ is the phase lag of dissipation with height z, ω is the tidal angular frequency, and A_z is constant vertical eddy viscosity. For rectilinear tidal flows, Eq. (1) gives a satisfactory description of the phase lag of dissipation with height (see Souza et al., 2004). Nevertheless, several complications appear when this formulation is applied to the rotating (i.e. with large magnitude of the ratio of minor to major axis for tidal ellipse) tidal BBL flows. First, the phase lags of turbulent dissipation, shear production and squared mean shear need to be intercompared straightforwardly in the rotating tidal flow. Using the variance method developed by Lu and Lueck (1999a, 1999b) and Stacey et al. (1999), the vertical profile of shear production can be estimated from high-frequency acoustical doppler current profiler (ADCP) surveys. Hence, it is possible to compare the ADCP-based shear production with the dissipation from turbulent microstructure profiling (see, Rippeth et al., 2003; Korotenko et al., 2013). Second, it is still unknown how the Coriolis effect adjusts the phase lag of dissipation in the rotating tidal flow. Third, the assumption of constant eddy viscosity over the water column needs to be carefully verified in describing the phase lag of dissipation with height.

The objective of this study is to investigate the phase lag of turbulent quantities with height in the rotating tidal flow. We will examine the temporal and vertical variability of turbulent quantities in the rotating tidal flow, and clarify the relationship of phase lag profiles among squared mean shear, turbulent dissipation and shear production. Moreover, we will develop simple theoretical formulations to describe the phase-lag development in the rotating tidal flow, and to clarify the main factors in the phase-lag growth.

2. Theory of tidal Ekman bottom boundary layer

By adopting the hydrostatic approximation, and neglecting the advective transport and horizontal diffusion of momentum, the governing equations for the rotating tidal flow in unstratified fluid are

$$\frac{\partial u}{\partial t}-fv+g\frac{\partial \eta}{\partial x}=\frac{1}{\rho}\left(\frac{\partial}{\partial z}(A_z\frac{\partial u}{\partial z})\right), \tag{2}$$

$$\frac{\partial v}{\partial t}+fu+g\frac{\partial \eta}{\partial y}=\frac{1}{\rho}\left(\frac{\partial}{\partial z}(A_z\frac{\partial v}{\partial z})\right), \tag{3}$$

where f is the Coriolis parameter, g is the gravitational acceleration, η is sea surface elevation relative to the equilibrium sea surface, and A_z is vertical eddy viscosity. The flow velocities (u, v) indicate two horizontal velocity components in (x, y) plane, and z denotes a vertical coordinate with an origin at the sea floor and is positive upwards, and t is time.

A crucial question in the above momentum balance is how to specify the vertical structure of eddy viscosity. The easiest method is to assume a constant value of eddy viscosity throughout the water column. With this constant viscosity, the analytical formulation for the rotating tidal flow with bed friction was earlier derived (Sverdrup, 1926; Munk et al., 1970; Kundu et al., 1981; Prandle, 1982). In particular, a simple solution has been achieved by Maas and Van Haren (1987) under the assumption of the linear bottom friction and the frictionless surface condition. When the tidal frequency (ω) is larger than the Coriolis parameter (f), the solutions given by Maas and Van Haren (1987) are

$$R^{+}=-\frac{G^{+}}{i(f+\omega)}\left(1-\frac{\cosh(\alpha(h-z))}{\cosh(\alpha h)+\frac{\alpha\cdot A_Z}{s}\sinh(\alpha h)}\right), \tag{4a}$$

$$R^{-}=-\frac{G^{-}}{i(\omega-f)}\left(1-\frac{\cosh(\beta(h-z))}{\cosh(\beta h)+\frac{\beta\cdot A_Z}{s}\sinh(\beta h)}\right), \tag{4b}$$

where

$$\alpha=(1+i)\sqrt{\frac{f+\omega}{2A_z}},$$

$$\beta=(1-i)\sqrt{\frac{\omega-f}{2A_z}},$$

$$s=C_d\frac{8}{3\pi}R_0,$$

and

$$R^{+}+R^{-}=u+vi,$$

in which R_0 denotes the amplitude of tidal currents at the bottom, C_d is the bed drag coefficient. $G^{\pm}$ are the rotating components of the horizontal pressure gradient divided by fluid density, $R^{\pm}$ are the rotating components of tidal velocity, and A_z is the vertical eddy viscosity. Here the superscripts of plus and minus represent the counterclockwise and clockwise rotating motions, respectively.

3. Field observations and data processing

3.1. Field campaign

Field measurements of mean flow and turbulence, water temperature and salinity were concurrently conducted in the southern Yellow Sea in the spring tide during 19th–20th September 2015. A mooring site with the mean water depth of 27 m (Fig. 1) was selected to examine the rotating tidal flow. The local weather conditions during the field survey were observed by a ship-borne automatic weather station.

An upward-looking 1200-kHz RDI Workhorse ADCP was deployed on a benthic-mounted tripod to observe mean and turbulent velocities in the tidal BBL. The ADCP sensor records the along-beam velocity with a ping rate of 2 Hz. A bin size was set to be 0.5 m and an ensemble-averaged velocity was taken in one second. The ADCP sensor was set in a standard RDI mode 1 in which the ambient noise was assumed to be independent of the measuring velocities (RDI, 1998). With an ambiguity velocity of 1.75 m s^{-1}, the standard deviation of uncertainty for each horizontal velocity was estimated to be 0.049 m s^{-1}. Besides the measurements of the flow velocity, the pressure sensor of the ADCP was used to obtain the height of wind waves during a 30-min interval at a 1-Hz sampling rate.

During the ADCP measurements, a series of vertical profiles of turbulence dissipation over the whole water column was taken using the turbulence microstructure profiler MSS-90L. The MSS-90L is equipped with fast response sensors of temperature, conductivity and two fine-scale velocity shear sensors (Prandke and Stips, 1998). The

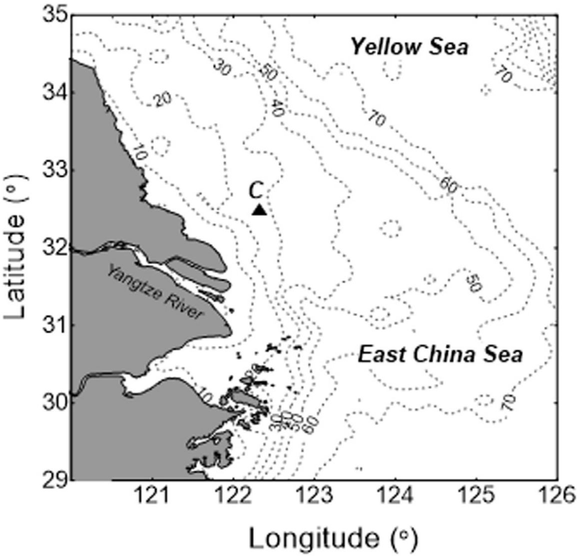

Fig. 1. The observation site in the southern Yellow Sea. Water depths (dash lines) are in meters.